CHAPTER 12

STELLAR ENGINES AND THE CONTROLLED MOVEMENT OF THE SUN

VIOREL BADESCU[1] AND RICHARD BROOK CATHCART[2]

[1] *Candida Oancea Institute, Polytechnic University of Bucharest, Spl. Independentei 313, Bucharest 79590, Romania;*

[2] *Geographos, 1300 West Olive Avenue, Burbank, CA 91506, USA*

Abstract: A stellar engine is defined in this chapter as a device that uses the resources of a star to generate work. Stellar engines belong to class A and B when they use the impulse and the energy of star's radiation, respectively. Class C stellar engines are combinations of types A and B. Minimum and optimum radii were identified for class C stellar engines. When the Sun is considered, the optimum radius is around 450 millions km. Class A and C stellar engines provide almost the same thrust force. A simple dynamic model for solar motion in the Galaxy is developed. It takes into account the (perturbation) thrust force provided by a stellar engine, which is superposed on the usual gravitational forces. Two different Galaxy gravitational potential models were used to describe solar motion. The results obtained in both cases are in reasonably good agreement. Three simple strategies of changing the solar trajectory are considered. For a single Sun revolution the maximum deviation from the usual orbit is of the order of 35 to 40 pc. Thus, stellar engines of the kind envisaged here may be used to control to a certain extent the Sun movement in the Galaxy

Keywords: stellar engine, Kardashev type II civilization, Shkadov thruster, Dyson sphere, galaxy gravitational potential, Sun movement control strategy

1. INTRODUCTION

For various reasons, mankind may be faced in the future with the problem of changing the Sun revolution motion. Avoiding nearby supernovae or ordinary star collisions are examples. Diffuse matter clouds could also be a potential danger. Some studies suggest that during its lifetime the Sun has suffered about ten

V. Badescu et al. (eds.), Macro-Engineering: A Challenge for the Future, 251–279.

encounters with major molecular clouds (MMC) and it has had close (impact parameter less than 20 pc) encounters with more than 60 MMC of various masses (Clube and Napier, 1984; Napier, 1985). These events induce perturbations of the Oort comet cloud, known to be sensitive to the particular galactic orbit of the Sun, leading to possible comet impacts on Earth (Gonzalez, 1999).

The Sun will steadily leave the main sequence in a few billion years, as stellar evolution calculations show (see e.g. Sackmann et al., 1993). The consequences will be a "moist greenhouse" effect on Earth, which will likely spell a definite end to life on our planet well before the Sun will become a Red Giant (Kasting, 1988; Nakajima et al., 1992). A preliminary solution to preserve the present-day climate on Earth may be to change its orbit. This subject is treated in detail in literature (see, e.g. Korykansky et al., 2001; McInnes, 2002) and in Chapter 11 of this book.

Zuckerman (1985) estimates that if ancient extraterrestrial civilizations exist in the Galaxy, then between 0.01 and 0.1 of them would have been forced to vacate their native planet due to the primary star leaving the main sequence. Problems with feasibility and dynamics of mass interstellar migrations (Jones, 1981; Newman and Sagan, 1981) prompted some researchers to propose the so-called "interstellar transfer" (or "solar exchange") solution (Hills, 1984; Shkadov, 1987; Fogg, 1989). In this case the Earth (or, more generally, the home planet) is to be transformed into a planet of a different star. The interstellar transfer requires first of all a way of controlling Sun (or star) movement in the Galaxy.

In this chapter we study the amplitude of a possible human intervention on Sun revolution motion. In section 2 we give a brief overview of different proposals in the literature. Also, we define the concept of stellar engine and we give details about various stellar engine classes. In section 3 we give the background physics associated to these devices. In section 4 we develop a model for the motion of the Sun in the Galaxy, based on usual Newtonian dynamics. The details of Sun movement are complex but an "average" motion can be defined by using appropriate global Galaxy gravitational potentials. The movement is then studied in both the normal (unperturbed) case and in the perturbed case, when an additional (stellar engine) thrust force is acting on the Sun. To increase the confidence in results, two different global gravitational potentials are used. Finally, in the Conclusion section we summarize the main findings of our work.

2. PROPOSALS TO CHANGE SUN MOTION

In his 12 May 1948 Halley Lecture at Oxford University in the UK, Fritz Zwicky (1889–1974) (see Zwicky, 1957) announced the possibility of

"... accelerating ... (the Sun) to higher speeds, for instance 1000 km/s directed toward Alpha Centauri A in whose neighborhood our descendents then might arrive a thousand years hence. [Such a one-way trip] ... could be realized through the action of nuclear fusion jets, using the matter constituting the Sun and the planets as nuclear propellants".

Zwicky's Halley Lecture, which may be seen as a response to the 16 July 1945 first nuclear fission explosion in the USA, was published in *The Observatory* (68:121–143, 1948) where the author merely hinted at the technical possibilities. At that time lasers were yet to be invented—*circa* 1960—and the controlled movement of asteroids and planets was still to be scientifically theorized (Korykansky, 2004). However, during 1971 when SCIART, a blend of "Science" and "Art", was organized by Bern Porter (1911–2004) even artists started to advocate use of nuclear particle beams for peaceful projects. By 1992, the artist Francisco Infante voiced his desire that humans redesign the firmament by intentionally shifting the positions of the stars other than the Sun (Infante, 1992).

The first scientifically recorded evidence of a natural celestial body in space colliding with the Sun came on 30-31 August 1979 when a cometary nucleus (1979 XI: Howard-Koomen-Michels) was observed as it vaporized in the Sun's corona.

At the Conference on Interstellar Migration (held at Los Alamos, New Mexico, in May 1983), David Russell Criswell extrapolated from available astronomical facts that the Sun might never enter a Red Giant-stage because it will be transformed into a stable White Dwarf-stage star via anthropogenic "star lifting". Criswell speculated about, perhaps proposed, a nameless macro-project the goal of which was to annually remove $6.5 \cdot 10^{18}$ tons of solar plasma from the Sun for a period of ~300 million years—about 2% of the Milky Way Galaxy's estimated age—setting aside the evicted plasma to cool by storing it near the Sun's poles in a stable form. He foresaw this macro-engineering activity commencing *circa* AD 2170–5650. Criswell's polar solar plasma lifts would be controlled and sustained versions of the Sun's natural coronal mass ejections, which occur most everywhere on that glowing celestial body's turbulent surface. Criswell's technique could be adapted to spin-up the Sun, thus causing a mixing of its materials artificially. However, a too rapid equatorial rotation could force the Sun to become dangerously unstable. Criswell did not mention moving stars in his work. His stellar husbandry and star lifting concepts essentially involved mining stars in order to divide their mass into smaller units so as to greatly extend their main sequence lifetime and the efficiency with which their radiant energy could be utilised. It was Fogg (1989) who adapted star lifting to moving stars by accelerating mass from just one stellar pole rather than both.

Oliver Knill, in 1997, suggested deliberate triggering of asymmetric fusion and fission in the Sun might be utilized to move the Sun and its cortege of planets (Knill, 2003). He referred to solar flares, both natural and man-made, as "rockets on the Sun". He alleged that if all the Sun's wind were focused in only one direction instead of being emitted globally, then the Sun might, in principle, be accelerated to a speed of 100 m/s in a year's time. Since such total harnessing of the Sun is unlikely, Knill offered that giant solar flares might be induced which would have the effect of propelling the Sun in a selected direction through space. His technical preference was to trigger huge artificial solar flares at one of the Sun's poles that perform as rocket motors, lest the induced anthropogenic solar wind cause Earth serious problems of human health or civilization's infrastructure breakdowns.

Of course, this limits the trajectory of the Sun to flight courses that may not be what human civilization most wants or needs. Like Fritz Zwicky, Knill opted for the use of nuclear particle beams as a tool of rocket motor ignition.

Zwicky, Knill and Criswell, therefore, have proposed very advanced tele-mining macro-projects that can have the planned effect of moving the Sun in some desired direction (Fogg, 1989).

Another way of controlling the Sun's movement is based on the concept of *stellar engine*. A stellar engine was defined in Badescu and Cathcart (2000) as a device that uses a significant part of a star's resources to generate work. Three types of stellar engines were identified and denoted as class A, B and C, respectively.

A class A stellar engine uses the impulse of the radiation emitted by a star to produce a thrust force. When acting through a finite distance the thrust force generates work. As example of class A stellar engine we refer to the Sun thruster proposed in Shkadov (1987), which consists of a mirror placed at some distance from the Sun (Fig. 1a). The mirror is situated such that the central symmetry of the solar radiation in the combined mirror-Sun system is violated and, as a consequence, a certain thrust force will arise. For a mirror of given surface mass density a balance exists between the gravitational force and the force due to solar radiation pressure at a certain mirror-Sun distance which remains constant. It may be shown that the equilibrium does not depend on the distance between mirror and the Sun, since both the gravitational force and the force of the solar light pressure per unit mirror surface are inversely proportional to the square of the radius. A mirror with given geometry located at 150 million km from the Sun requires a surface mass density of about $1.55 \cdot 10^{-3}$ kg/m^2 while its total mass amounts $10^{19} - 10^{20}$ kg (which may be compared with the mass of the Earth, which is $5.977 \cdot 10^{24}$ kg). Detailed calculations may be found in Shkadov (1987).

A class B stellar engine uses the energy flux of the radiation emitted by a star to generate mechanical power. An example of class B stellar engine was proposed in Badescu (1995). It consists of two concentric spherical "shells" centered on the star. The "shells" have not necessarily continuous boundaries but they could be as well as imaginary envelopes of a very large number of smaller 3D bodies englobing the star. The inner surface acts as a solar energy collector. The outer surface is a thermal radiator. The two surfaces have different but rather uniformly distributed temperatures, T_p and T_r, respectively. The existing difference of temperature $T_p - T_r$ determines a heat flux from the inner towards the outer surface. This flux entering the thermal engine is used for power generation.

A class C stellar engine was defined in Badescu and Cathcart (2000) as a combination of a class A and class B stellar engine (Fig. 1b). It uses the impulse and the energy of the star radiation to provide both a thrust force and mechanical power for its owning civilization. Note that class B and C stellar engines are normally built by using the material of the inner planets (see Section 2.2). Of course, in this case the entire human population has to leave the Earth and move on the stellar engine.

For completeness here we define a new stellar engine as follows. A class D stellar engine uses a star's mass to propel the star. A particular class D stellar engine is

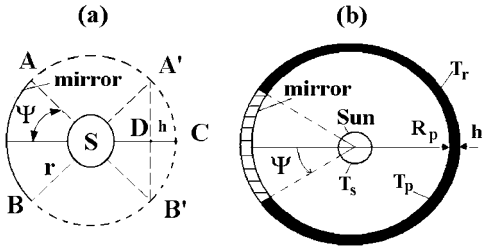

Figure 1. (a). A class A stellar engine (Shkadov thruster). r – distance between star S and the mirror. Ψ – mirror rim angle. (b). The class C stellar engine proposed in Badescu and Cathcart (2000). R_p – distance between star and inner surface, h – distance between inner and outer surfaces, T_S – star temperature; T_p, T_r – temperatures of the inner and outer surfaces, respectively

the stellar rocket described in Fogg (1989), based on a modification of the concept of "star lifting" proposed in Criswell (1985).

3. THERMODYNAMICS OF STELLAR ENGINES

3.1 Class A Stellar Engines

The energy radiated by a star is due to the nuclear reactions taking place in the nucleus. A steady-state star is characterized by a permanent balance between the energy flux generated during the nuclear reactions and the energy flux emitted at star's surface in all directions.

The bolometric luminosity $\tilde{L}_S$ of the Sun (i.e. its energy radiated on all wavelengths per unit time) is in present times (Ureche, 1987, p. 102):

$$\tilde{L}_S = 3.826 \cdot 10^{26} \text{ W}. \tag{1}$$

Let us consider the class A stellar engine of Fig. 1a. The star is prevented from losing energy on the solid angle covered by the mirror, as the energy emitted on that direction is returned to the star together with the reflected radiation. As the nuclear reaction rate doesn't change, the same energy flux $\tilde{L}_S$ has to be dissipated in space but this time from the effective (not covered by the mirror) star surface only. Consequently, the photosphere temperature will increase and it is expected that the star will change gradually to a different steady state. This effect was neglected in Shkadov (1987).

One denotes by R_S and $\tilde{T}_S$ the Sun's ray and its present-day temperature, respectively. The area of the Sun surface (S_S) and the surface of the Sun covered by the mirror ($S_{S,\text{covered}}$) are, respectively (Fig. 1a)

$$S_S = 4\pi R_S^2 \tag{2}$$

$$S_{S,\text{covered}} = 2\pi R_S h \tag{3}$$

Here h can be easily computed as a function of the mirror rim angle Ψ

$$h = R_S(1 - \cos\Psi). \tag{4}$$

The effective (not covered by the mirror) Sun surface area, $S_{S,eff}$, is:

$$S_{S,eff} = S_S - S_{S,\mathrm{covered}}. \tag{5}$$

One supposes the Sun is a blackbody, both before and after mirror installation. Then the steady-state Sun temperature after mirror installation (T_S) has to obey the following energy balance equation:

$$\tilde{L}_S = S_S \sigma \tilde{T}_S^4 = S_{S,eff}\sigma T_S^4. \tag{6}$$

By using Eqs. (5) and (6) one obtains

$$T_S = \frac{\tilde{T}_S}{\left(1 - S_{S,\mathrm{covered}}/S_S\right)^{1/4}}. \tag{7}$$

Using Eqs. (2)–(4) and Eq. (7) allows us to obtain the dependence of the Sun's temperature T_S on the mirror rim angle Ψ. Results are shown in Fig. 2. By increasing the mirror's rim angle the spectral class of the Sun gradually changes from G2 towards F2 (Harvard classification).

The increase in the Sun's photosphere temperature is accompanied by a change in its present absolute bolometric magnitude $\tilde{M}_b$. This change is governed by the equation (see Eq. (5.23) in Ureche, 1987, p. 109):

$$M_b = \tilde{M}_b - 10\lg\left(\frac{T_S}{\tilde{T}_S}\right). \tag{8}$$

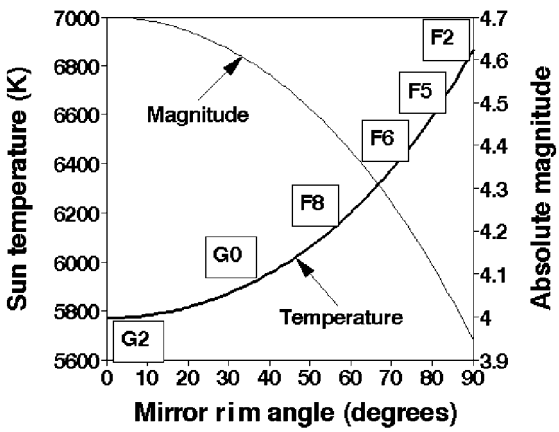

Figure 2. Dependence of Sun's photosphere temperature T_s and absolute magnitude M_b on the mirror rim angle Ψ (see Fig. 1a). The relation between temperature and star spectral classes (Harvard classification) is also shown

Figure 2 shows the dependence of the absolute bolometric magnitude of the Sun, M_b, as a function of mirror rim angle Ψ. We have taken into account that the Sun's present absolute bolometric magnitude is $\tilde{M}_b = 4.7$.

One can see that for the rim angle considered by Shkadov (1987) in his calculations (i.e. $\Psi = 30°$) both the photosphere temperature T_S (and its associated spectral class) and the absolute bolometric magnitude M_b remains quite close to the present-day values.

The mass of the mirror is distributed over a very large surface and, as a consequence, its influence on the orbit of the Earth is expected to be small. However, the Earth temperature may be affected in case of mirrors with large rim angle. Therefore, the mirror should be placed and kept in such a position that the orbit and temperature of the Earth are not affected significantly (for example, the mirror-Sun direction may be kept perpendicular on Earth orbit).

3.2 The Dyson Sphere Revisited

In this section we shall consider a 'usual' thin Dyson sphere (DS) englobing the Sun (Dyson, 1966). The inner DS surface constitutes the habitat of mankind. Due to its symmetry, the Dyson sphere will have a rather uniform surface temperature. The DS material is assumed to have a good thermal conductivity. Consequently, one could neglect the thermal gradients on material's thickness.

The steady-state energy balance per unit DS area is:

$$a\frac{B_S}{\pi}\sigma T_S^4 + a(1-\frac{B_S}{\pi})e_{\text{int}}\sigma T_p^4 = (e_{\text{int}} + e_{ext})\sigma T_p^4. \tag{9}$$

Here a is the absorptance of DS inner surface while e_{int} and e_{ext} is the emittance of DS inner and outer surfaces, respectively. Also, T_S and T_p is Sun and DS temperature, respectively. The first term in the l.h.s. of Eq. (9) is the energy flux density absorbed from the Sun while the second term is the energy flux density absorbed from the whole Dyson sphere. The r.h.s. of Eq. (9) contains the energy flux densities emitted by the DS inner and outer surfaces, respectively.

The geometric factor B_S in Eq. (9) may be computed as in Landsberg and Badescu (1998):

$$B_S = \int_0^{\delta} \cos\theta \sin\theta d\theta \int_0^{2\pi} d\alpha = \pi \sin^2\delta, \tag{10}$$

where δ is the half-angle of the cone subtended by the Sun when viewed from an arbitrary point placed on DS inner surface. One can simply prove that

$$\sin^2\delta = \left(\frac{R_S}{R_p}\right)^2, \tag{11}$$

where R_S and R_p are Sun and DS radii, respectively. One denotes:

$$x \equiv \frac{B_S}{\pi} = \left(\frac{R_S}{R_p}\right)^2. \tag{12}$$

The steady-state energy balance for the Sun's surface is:

$$4\pi R_S^2 \sigma T_S^4 - 4\pi R_p^2 e_{\text{int}} \sigma T_p^4 = \tilde{L}_S. \tag{13}$$

The first term in the r.h.s. of Eq. (13) is the energy flux emitted by the whole surface of the Sun while the second term is the energy flux received by the whole surface of the Sun from the Dyson's sphere. If one takes into account, on one hand, the multiple reflections of solar radiation on DS inner surface, and, on the other hand, the DS symmetry, one concludes that the absorptance $a \approx 1$. This is only true if one neglects that part of the radiation reflected by DS inner surface which is incident on the Sun's surface. By solving the Eqs. (9) and (13) and taking into account Eq. (12) one obtains:

$$T_p = \left(\frac{\tilde{L}_S}{4\pi R_p^2 \sigma e_{ext}}\right)^{1/4} \tag{14}$$

$$T_S = \left[\left(1 + x\frac{e_{\text{int}}}{e_{ext}}\right)\frac{\tilde{L}_S}{4\pi R_S^2 \sigma}\right]^{1/4}. \tag{15}$$

These relations are valid under the condition $T_S > T_p$, which may be re-written (by using Eqs. 12, 14 and 15) as:

$$R_p \geq \left(\frac{1 - e_{\text{int}}}{e_{ext}}\right)^{1/2} R_S. \tag{16}$$

Figure 3 of Badescu and Cathcart (2000) shows the dependence of DS temperature T_p on the radius for various values of DS surface emittance $e = e_{\text{int}} = e_{ext}$. A surface temperature comparable with present-day average ground surface temperature (∼300 K) corresponds to high values of surface emittance. A number of conclusions may be drawn. First, small radii increase the feasibility of a DS project as the amount of material required is proportional to R_p^2. Second, the inner planets seem to be the best source of material in this case due to the shorter distance between their orbit and the place of the future Dyson sphere. The material of the inner planets has a relatively low albedo (between 0.07 in case of Mercury and 0.39 in Earth case (Moore, 1970); Venus' high albedo is due to its cloudy atmosphere). Normally, low albedo values are associated to surfaces with high absorptance (or, which equivalent due to Kirchoff's law, to surfaces with high emittance). Therefore, the inner planets are appropriate for DS building also from the point of view of their optical properties.

3.3 Class B and Class C Stellar Engines

Due to mirror's imperfect reflection and to the finite size of the Sun, a spot of concentrated light is expected to appear on the inner surface of class B and class C stellar engines in its part opposite to the mirror. This spot is associated with a temperature peak and can be used to increase locally the work rate provided by the thermal engine. However, for convenience we shall assume: (i) the Sun has a negligible size as compared to the radius of the stellar engine and (ii) the mirror is perfect (i.e. the mirror has a unity reflectance and it reflects all the incident rays on Sun's direction). As a consequence, the mirror temperature is very low and is not considered in this work.

Now, we shall analyze a region on the inner surface of the class B stellar engine (or on that part of the class C stellar engine that is used for power generation). The steady-state energy balance per unit area of the inner surface is:

$$q_H = \frac{B_S}{\pi}\sigma\ T_S^4 + \left(1 - \frac{B_S}{\pi}\right) e_{\text{int}}\sigma\ T_p^4 - e_{\text{int}}\sigma\ T_p^4. \tag{17}$$

Here, q_H is the energy density flux entering the thermal engine (Fig. 3). The first and the second terms in the r.h.s of Eq. (17) is the energy flux density absorbed from the Sun and from the whole stellar engine inner surface, respectively. Here, the conservation of the etendue on the mirror surface is taken into account (see e.g. Badescu, 1993, and references therein). The third term in the r.h.s of Eq. (17) is the energy flux density emitted by the stellar engine's inner surface.

The energy balance per unit area of the outer surface is:

$$q_L = e_{ext}\sigma\ T_r^4. \tag{18}$$

In Eq. (18) q_L is the energy flux density leaving the thermal engine per unit surface area while T_r is the temperature of the outer surface of the stellar engine.

Here a particular case of endoreversible thermal engine is considered, namely the Chambadal-Novikov-Curzon-Ahlborn engine (CNCA engine for short). It consists of three parts (Fig. 3):

(a) a reversible part working between two heat reservoirs (one at the high temperature), say t_1, and one at the low temperature, say t_2; (usually, t_1 and t_2 are the temperatures of the working fluid during its isothermal expansion and compression, respectively).

(b) two irreversible parts containing temperature drops (i.e. the temperature fall $T_p - t_1$ accompanying q_H and the temperature fall $t_2 - T_r$ accompanying q_L). A linear relationship exists between the heat flows and the temperature gradients.

Details on endoreversible and CNCA engines may be found in the reviews by Bejan (1996) and Hoffmann et al., (1997).

The entropy balance for the CNCA engine is (De Vos, 1985):

$$\frac{q_H}{T_p^{1/2}} + \frac{q_L}{T_r^{1/2}} = 0. \tag{19}$$

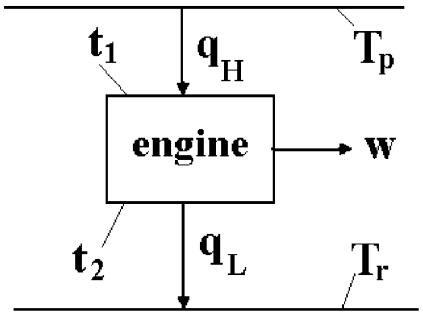

Figure 3. Power generation by using a CNCA thermal engine. q_H, q_L – heat fluxes entering and leaving the thermal engine, respectively; t_1 and t_2 – the absolute temperatures of the working fluid in contact with the two heat reservoirs. T_p, T_r – temperatures of the inner and outer surfaces, respectively; w – work rate (power)

The energy balance for the whole surface of the Sun is:

$$S_{S,eff}\sigma T_S^4 - S_S e_{\text{int}}\sigma T_p^4 = \tilde{L}_S. \tag{20}$$

The first term in the l.h.s. of Eq. (20) is the energy flux lost by the Sun; it takes into consideration that all the energy emitted by the Sun on mirror's direction is reflected back. The second term in the l.h.s. of Eq. (20) is the energy flux received by the Sun from the inner surface of the stellar engine. It takes into account that, due to the perfect mirror, each unit surface area of the Sun receives the energy flux density $e_{\text{int}}\sigma T_p^4$.

Simple computation shows that:

$$S_{S,eff} = S_S \frac{1+\cos\Psi}{2}. \tag{21}$$

One uses the following notation:

$$\theta_S \equiv \frac{T_S}{\tilde{T}_S} \qquad \theta_p \equiv \frac{T_p}{\tilde{T}_S} \qquad \theta_r \equiv \frac{T_r}{\tilde{T}_S}. \tag{22}$$

In the following θ_p is supposed to be known. This is a reasonable assumption as normally T_p should allow living conditions and consequently has a small variation range. By using Eqs. (12) and (17)–(22) one derives:

$$\theta_S = \left(e_{\text{int}}\theta_p^4 + \frac{2}{1+\cos\Psi}\right)^{1/4} \tag{23}$$

$$\theta_r = \left(\frac{2}{1+\cos\Psi}\frac{x}{e_{ext}}\frac{1}{\theta_p^{1/2}}\right)^{1/4}. \tag{24}$$

The two following conditions have to be fulfilled: $\theta_S > \theta_p$ and $\theta_p > \theta_r$, in order for the thermal engine to operate (i.e. to generate a positive power). By using Eqs. (22)–(24) these conditions turn out to be:

$$e_{\text{int}} \geq 1 - \frac{2}{\theta_p^4 (1 + \cos \Psi)} \tag{25}$$

$$R_p \geq R_S \left[\frac{2}{e_{ext} \theta_p^4 (1 + \cos \Psi)} \right]^{1/2}. \tag{26}$$

The constraint Eq. (25) is always fulfilled as its r.h.s. member is non-negative, because $\theta_p < 1$ (see Eq. 22) and $\cos \Psi \leq 1$. On the other hand, Eq. (26) gives a minimum limit for the radius of the stellar engine.

Let us have a look to the class B stellar engine proposed in Badescu (1995). It may be seen as a particular case of class C stellar engine (it corresponds to a missing mirror or, in other words, to $\Psi = 0°$). For an outer surface emittance $e_{ext} = 1$ one finds the minimum radius $R_{p,\min} = R_S/\theta_p^2$. This is very close to the result $R_{p,\min} = R_S(1 - \theta_p^4)^{1/2}/\theta_p^2$ derived in Badescu (1995) without taking into account that the presence of the stellar engine increases the Sun's temperature.

Figure 5 of Badescu and Cathcart (2000) shows the dependence of the Sun temperature T_S on the mirror rim angle Ψ and the radius R_p of the stellar engine. Generally, T_S increases with increasing Ψ and the radius R_p. However, this applies mainly for $R_s < 400 \cdot 10^6$ km.

Figure 4a shows the dependence of the outer surface temperature T_r on Ψ and R_p. Generally, T_r decreases by increasing R_p and decreasing the mirror rim angle Ψ.

Knowledge of the temperature T_r is important in case of searching for extraterrestrial intelligence (SETI). Indeed, it is (practically) the only information that outside world receives from a Kardashev type II civilisation. One reminds that according to the classification proposed by Kardashev a technological civilisation is of type I, II or III if it has under its control the materials and energy resources of a planet, star, or galaxy, respectively (see Kardashev, 1964; Badescu and Cathcart, 2000). From Fig. 4a one learns that galactic IR sources corresponding to temperatures lower than 300 K should not be overlooked during SETI activities. For more information about the thermal signature of possible extraterrestrial civilizations in the Galactic context see Chapter 13 in this book.

The heat flux density q_H is obtained by using Eqs. (12), (17), (22)–(24):

$$q_H = x \sigma \tilde{T}_S^4 \frac{2}{1 + \cos \Psi}. \tag{27}$$

The well-known CNCA efficiency is (De Vos, 1985)

$$\eta_{CNCA} = 1 - \left(\frac{T_r}{T_p} \right)^{1/2} = 1 - \left(\frac{\theta_r}{\theta_p} \right)^{1/2}. \tag{28}$$

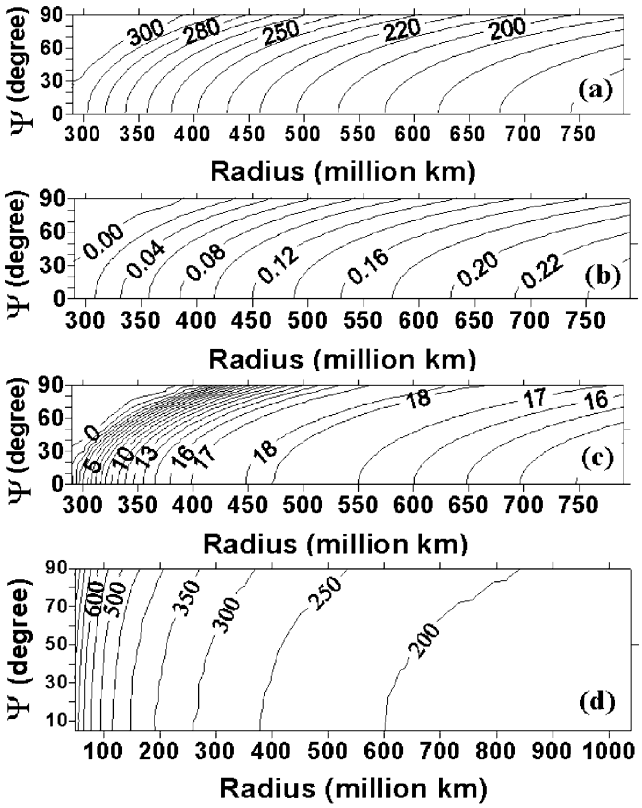

Figure 4. Dependence of various quantities on mirror rim angle Ψ and radius R_p in case of a class C stellar engine. (a) Outer surface temperature T_r (K); (b) Thermal engine efficiency η_{CNCA}; (c). Power density w_{CNCA} (W/m^2); (d) Optimum inner surface temperature T_p (K). In cases (a), (b), (c) the temperature of the inner surface is $T_p = 300$ K and the emittance of both inner and outer surfaces is $e_{int} = e_{ext} = 0.8$. In case (d) $e_{int} = e_{ext} = 1$

Figure 4b show the dependence of η_{CNCA} on Ψ and R_p. This performance indicator increases by increasing the radius R_p and decreasing the mirror rim angle Ψ. One can see that the efficiency vanishes and tends to become negative for R_p values smaller than the limit predicted by Eq. (26) (see the top left corner of Fig. 4b, where the associated "critical" rim angle may be easily evaluated). Generally, η_{CNCA} is smaller than the efficiency (which may exceed 0.5) of common terrestrial power plants working at large temperature differences but it is comparable with the efficiency of Stirling engines working at small differences of temperature (tens of Kelvin)(see Badescu, 2004).

Figure 8 of Badescu and Cathcart (2000) shows the dependence of η_{CNCA} on the outer surface emittance e_{ext}. The efficiency increases by increasing e_{ext}. This can be explained as follows. Increasing the emittance e_{ext} makes the temperature T_r decrease (see Fig. 5) and this finally leads to an increase in the efficiency. This has

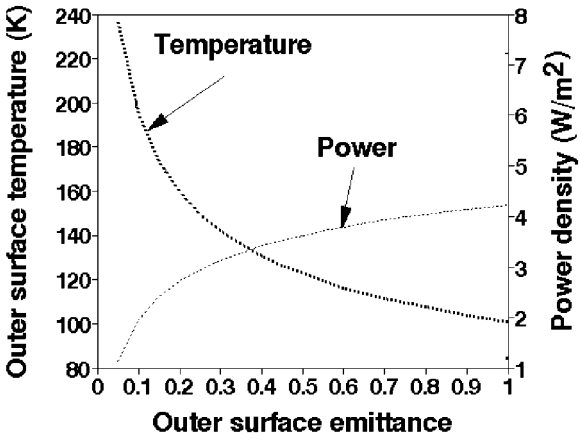

Figure 5. Dependence of the power density w_{CNCA} and of the outer surface temperature T_r on the outer surface emittance e_{ext} in case of a class C stellar engine. $R_p = 300$ millions km and $\Psi = 30$ degrees. Other inputs as in Fig. 4a

again consequences for SETI activities. Indeed, the thermal signature of possible extraterrestrial civilizations may be at a lower level than commonly expected.

The work rate (power) density w_{CNCA} is given by:

$$w_{CNCA} = q_H \eta_{CNCA}. \tag{29}$$

Figure 4c shows that for small R_p values the power density w_{CNCA} decreases by increasing the mirror rim angle Ψ. However, at high R_p values the reverse happens. There is a maximum maximorum power density which corresponds in both cases to a R_p radius of about $450 \cdot 10^6$ km. This means that there is an optimum stellar engine radius. That optimum radius is obviously larger than the radius of commonly proposed Dyson spheres, which is of the order or Earth orbit radius. One can notice that for some values of R_p and Ψ the power density w_{CNCA} becomes negative (left top corner of Fig. 4c).

Figure 5 shows the dependence of the power density w_{CNCA} and of the temperature T_r on the emittance of the outer surface e_{ext}. As expected, the temperature T_r decreases by increasing e_{ext}. But decreasing T_r leads to an increase in the efficiency (see Fig. 8 of Badescu and Cathcart, 2000) and finally this is associated with an increase in the power density w_{CNCA}.

Practically, w_{CNCA} and T_r do not depend on the emittance of the inner surface e_{int}.

3.4 The Thrust Force Acting on the Sun

We showed in Section 3.1 that the presence of the mirror makes the Sun's temperature increase. This has consequences on the radiation impulse and finally on the thrust force acting on the Sun. In this section one evaluates the thrust force in case of both class A (Shkadov thruster) and class C stellar engines.

3.4.1 Class A stellar engine (Shkadov thruster)

The impulse of the radiation per unit time leaving the Sun is proportional to the energy emitted (see Shkadov, 1987):

$$p = \frac{S_S \sigma T_S^4}{c}. \tag{30}$$

By taking into account the Eqs. (5)–(7), (21) and (30) one obtains:

$$p = \frac{\tilde{L}_S}{c} \frac{2}{1+\cos\Psi}. \tag{31}$$

Note that in Shkadov (1987) the increase in Sun temperature due to mirror's existence is not considered and the following approximate relation is used: $p = \tilde{L}_S/c$.

The thrust force $\bar{f}$ per unit area in the direction of the normal $\bar{n}$ to an arbitrary unit area placed on the base surface of the spherical cone A'SB' of Fig. 1a is (see also Fig. 1 of Shkadov, 1987):

$$f = \frac{\tilde{L}_S}{c} \frac{2}{1+\cos\Psi} \frac{1}{4\pi R_p^2}. \tag{32}$$

When $\Psi = 0$, Eq. (32) reduces to Eq. (1) of Shkadov (1987). The correction factor $2/(1+\cos\Psi)$ takes into account the increase in Sun's temperature.

The thrust F being produced by the Sun-mirror system due to the non-symmetric radiation field is given by Shkadov (1987)

$$F = \int \bar{f} \cdot \bar{n}\tau \, dS, \tag{33}$$

where S is the base area of the spherical cone A'SB' in Fig. 1a while τ is the unit vector along the axis of that cone. After integration one obtains:

$$F = \frac{\tilde{L}_S}{2c}(1-\cos\Psi). \tag{34}$$

When $\Psi = 0$, Eq. (34) reduces to Eq. (2) of Shkadov (1987). The thrust force F increases by increasing the mirror rim angle Ψ, as expected. The original result is $4cF = \tilde{L}_S \sin^2\Psi$ (see Eq. 2 of Shkadov, 1987). One can see that our Eq. (34) generally estimates a higher thrust force, which, in the particular case $\Psi = 90°$, doubles the result obtained by using Eq. (2) of Shkadov (1987). The main consequence is the fact that the lateral deviation during one orbital period of the Sun, evaluated by Shkadov (1987) to about 4.4 parsec, is underestimated. The value estimated by Shkadov (1987) for the acceleration induced by the thrust force F on the solar system motion is $6.5 \cdot 10^{-13}$ m/s^2. This is half of the result obtained by using the improved model from this chapter. Both values have to be compared with the gravitational acceleration of the galactic field, which is about $1.85 \cdot 10^{-10}$ m/s^2 (Shkadov, 1987). One concludes that the magnitude of the disturbing force created by the sun-mirror system is small, as expected.

3.4.2 Class C stellar engine

The impulse of the radiation emitted by the inner surface of a class C stellar engine at temperature T_p impinging on the Sun, in case that no mirror exists, is:

$$p_D = \frac{4\pi R_S^2 e_{\text{int}} \sigma T_p^4}{c}. \tag{35}$$

By using the notations Eqs. (22) and Eqs. (23)-(24) one obtains:

$$p_D = \frac{\tilde{L}_S}{c} e_{\text{int}} \frac{\theta_p^4}{\theta_S^4}. \tag{36}$$

Consequently, the impulse of the net flux of radiation leaving the Sun is:

$$p_{net} = p - p_D. \tag{37}$$

By taking into account the Eqs. (35)–(37) one obtains:

$$p_{net} = \frac{\tilde{L}_S}{c} \left(1 - e_{\text{int}} \frac{\theta_p^4}{\theta_S^4}\right) \frac{2}{1+\cos\Psi}. \tag{38}$$

The thrust force f per unit area in the direction of the normal $\bar{n}$ to the base surface of the circular cone A'SB' (see Fig 1a) is:

$$f = \frac{\tilde{L}_S}{c} \left(1 - e_{\text{int}} \frac{\theta_p^4}{\theta_S^4}\right) \frac{2}{1+\cos\Psi} \frac{1}{4\pi R_p^2}. \tag{39}$$

The thrust force F is obtained after computing the integral in Eq. (33):

$$F = \frac{\tilde{L}_S}{2c} \left(1 - e_{\text{int}} \frac{\theta_p^4}{\theta_S^4}\right) (1-\cos\Psi). \tag{40}$$

Generally, the thrust force F increases by increasing the mirror rim angle Ψ. One has to remind, however, that increasing Ψ leads to a decrease in the efficiency η_{CNCA} (see Fig. 4b). Note that F is dependent on the temperature T_p via the dimensionless parameter θ_p. The optimum value of T_P which maximizes F is shown in Fig. 4d for $e_{\text{int}} = e_{ext} = 1$. Let us consider an optimum temperature $T_p \sim 300\ K$ (appropriate for common living conditions on Earth). Then $F$is a maximum for a radius R_p around 300 millions km.

In the next sections one shall need the thrust force F' per unit mass of the solar system. This implies dividing the Eqs. (34) and (40), respectively, by $M_S + M_{planets}$, where $M_S = 1.989 \cdot 10^{30}$ kg and $M_{planets} = 2.7 \cdot 10^{27}$ kg are Sun mass and the mass

of Solar System's planets, respectively. Then, the expressions of F' for class A and class C stellar engines are, respectively:

$$F'_A = \frac{\tilde{L}_S}{2c} \frac{1-\cos\Psi}{M_S + M_{planets}} \tag{41}$$

$$F'_C = \frac{\tilde{L}_S}{2c} \left(1 - e_{\text{int}} \frac{\theta_p^4}{\theta_S^4}\right) \frac{1-\cos\Psi}{M_S + M_{planets}}. \tag{42}$$

When used in case of the Sun, the Eqs. (41) and (42) lead to (practically) the same numerical results. This is due to the fact that $e_{\text{int}}(\theta_p/\theta_S) \propto (300/5760)^4$ is very close to zero. Consequently, the results reported below apply to both types of stellar engines and the indexes A or C will be removed for convenience.

4. CHANGE OF SUN MOVEMENT IN GALAXY

The Sun's galactic orbit is described here by ignoring the perturbations due to Galaxy spiral arms and the encounters with massive dust/molecular clouds. The gravitational forces acting on the Sun in the absence of a stellar engine are modeled as being derived from scalar potentials. Various gravitational potentials were proposed and studied in the relevant literature. It is not our aim to decide which of these potentials is more appropriate to be used in practice. Here we shall use the simple spherical potential adopted earlier by Shkadov (1987) (see section 4.1 below). However, some authors consider it to be helpful to decompose the Sun's motion into two orthogonal components: a motion in the galactic mid-plane and a motion perpendicular to the plane (Gonzalez, 1999). Therefore, a cylindrical gravitational potential will be used in Section 4.2. It is a generalization of a Plummer potential, previously used by Carlberg and Innanen (1987). We shall see that both potentials predict results of the same order of magnitude and this may act as a sort of cross-checking.

The stellar engine thrust force F is superposed on the Galaxy gravitational forces acting on the Sun. As a result, a *perturbed* Sun trajectory will result. It is the scope of the present section to evaluate the distance between the perturbed position and the Sun's usual (average) position.

4.1 Movement in Curvilinear Coordinates

A few results of vector analysis are used here to describe Sun motion. We define a cartesian system of coordinates $\{x^i\}$ $(i = 1, 2, 3)$ with the plane Ox^1x^2 in the equatorial plane of the Galaxy. The Sun movement in the Galaxy will be given by three parametric functions, say $x^i = x^i(t)$ $(i = 1, 2, 3)$. A curvilinear coordination system q^i $(i = 1, 2, 3)$ is then introduced. The transformation $\{x^i\} \to \{q^i\}$ defines a metric tensor g_{ij} $(i, j = 1, 2, 3)$. One denotes by $\dot{q}^i$ the usual first order time derivatives of the coordinates q^i $(i = 1, 2, 3)$. They are called *generalized* velocities. Note

that their dimensions are not necessarily length per time. The connection between $\dot{q}^i$ and the components of Sun's velocity v^i (i.e. the projections on the coordinates q^i $(i = 1, 2, 3)$) are given by the usual relationships (Beju et al., 1976, p 173):

$$v^i = H_i \dot{q}^i \qquad (i = 1, 2, 3)\,, \tag{43}$$

where H_i are the Lamé coefficients, which can be obtained by (Beju et al., 1976, p 172):

$$H_i = g_{ii}^{1/2} \qquad (i = 1, 2, 3)\,. \tag{44}$$

The contravariant time derivative D/Dt of the generalized velocities $\dot{q}^i$ is given by (Beju et al., 1976, p 183)

$$\frac{D\dot{q}^i}{Dt} = \frac{d\dot{q}^i}{dt} + \Gamma^i_{jk}\dot{q}^j\dot{q}^k, \tag{45}$$

where Γ^i_{jk} are Christoffel coefficients of the second kind. Here the Einstein convention for summation was used. The equations of movement of the Sun have the covariant form:

$$a^i = H_i \frac{D\dot{q}^i}{Dt} = G^i + F'^i \qquad (i = 1, 2, 3)\,, \tag{46}$$

where a^i is the i-th contravariant component of Sun's acceleration while G^i and F'^i are the i-th contravariant components of the gravitational force and of the stellar engine thrust, respectively, both of them per unit mass of the Solar System.

The Sun motion is described first by mean of the spherical coordinate system (R, λ, φ) used in Shkadov (1987). The change of coordinates $\left(x^1, x^2, x^3\right) \rightarrow (R, \lambda, \varphi)$ is:

$$x^1 = R\cos\varphi\cos\lambda \quad x^2 = R\cos\varphi\sin\lambda \quad x^3 = R\sin\varphi, \tag{47}$$

where $0 \leq \lambda \leq 2\pi$ and $-\pi/2 \leq \varphi \leq \pi/2$. The equatorial plane of the Galaxy is associated to $\varphi = 0$. Details about the metric tensor g_{ij}, the contravariant tensor g^{ij} $(i, j = R, \lambda, \varphi)$, the Lamé coefficients and the Christoffel symbols of first and second kind, respectively, may be found in Badescu and Cathcart (2006).

Use of Eqs. (43) allows to obtain the components v^i $(i = R, \lambda, \varphi)$ of Sun's velocity:

$$v^R = \dot{R} \quad v^\lambda = R\cos\varphi\dot{\lambda} \quad v^\varphi = R\dot{\varphi}, \tag{48}$$

while use of Eqs. (44)–(46) and (48) allow to obtain the components $\dot{v}^i$ (R, λ, φ) of Sun's acceleration:

$$\begin{aligned}
\dot{v}^R &= \frac{\left(v^\lambda\right)^2 + \left(v^\varphi\right)^2}{R} + G^R + F'^R \\
\dot{v}^\lambda &= -\frac{v^R v^\lambda - v^\lambda v^\varphi \tan\varphi}{R} + G^\lambda + F'^\lambda \\
\dot{v}^\varphi &= -\frac{v^\lambda v^\varphi + \left(v^\lambda\right)^2 \tan\varphi}{R} + G^\varphi + F'^\varphi
\end{aligned}\,. \tag{49}$$

The Sun motion is described now by mean of the cylindrical coordinate system (r, θ, z) used in Carlberg and Innanen (1987). The change of coordinates $\left(x^1, x^2, x^3\right) \to (r, \theta, z)$ is:

$$x^1 = r\cos\theta \quad x^2 = r\sin\theta \quad x^3 = z, \tag{50}$$

where $0 \leq \theta \leq 2\pi$. The equatorial plane of the Galaxy is associated to $z = 0$. Again, details about the metric tensor g_{ij}, the contravariant tensor g^{ij} $(i, j = r, \theta, z)$, the Lamé coefficients and the Christoffel symbols of first and second kind, respectively, may be found in Badescu and Cathcart (2006).

Use of Eqs. (43) allows to obtain the components v^i $(i = r, \theta, z)$ of Sun's velocity:

$$v^r = \dot{r} \quad v^\theta = r\dot{\theta} \quad v^z = \dot{z}, \tag{51}$$

while use of Eqs. (44)–(46) and (51) allow to obtain the components $\dot{v}^i$ (r, θ, z) of Sun's acceleration:

$$\begin{aligned} \dot{v}^r &= \frac{\left(v^\theta\right)^2}{r} + G^r + F'^r \\ \dot{v}^\theta &= -\frac{v^r v^\theta}{r} + G^\theta + F'^\theta \\ \dot{v}^z &= G^z + F'^z \end{aligned}. \tag{52}$$

The above theory will be used now in case of two Galaxy gravitational potentials.

4.2 First Galaxy Gravitational Potential

As a first axi-symmetrical gravitational potential per unit mass of the solar system, $\Phi(R, \lambda, \varphi)$, we shall adopt:

$$\Phi(R, \lambda, \varphi) = \frac{A}{B + \left(B^2 + R^2\right)^{1/2}} - \frac{C^2 \tan^2(\varphi/2)}{R^2\left(1 + D^2\tan^2(\varphi/2)\right)^{1/2}}. \tag{53}$$

Here a spherical system of coordinates (R, λ, φ) was used. The constants in Eq. (53) are as follows: $A = 3.18 \cdot 10^{22}\ \mathrm{km}^3/\mathrm{s}^2$, $B = 8.6 \cdot 10^{16}\ \mathrm{km}$, $C = 3.27 \cdot 10^{20}\ \mathrm{km}^2/\mathrm{s}$ and $D = 30.8$ (Shkadov, 1987).

The components of the gradient of Φ are projections of the gravitational acceleration vector G:

$$G^R = \frac{1}{H_R}\frac{\partial\Phi}{\partial R} \qquad G^\lambda = \frac{1}{H_\lambda}\frac{\partial\Phi}{\partial\lambda} = 0 \qquad G^\varphi = \frac{1}{H_\varphi}\frac{\partial\Phi}{\partial\varphi}. \tag{54}$$

Here the Lamé coefficients H_i $(i = R, \lambda, \varphi)$ were used.

One denotes the components of Sun's velocity by v^i $(i = R, \lambda, \varphi)$ and one defines the following dimensionless variables:

$$\tilde{t} \equiv \frac{t}{T_0} \quad \tilde{R} \equiv \frac{R}{r_0} \quad \tilde{v}^R \equiv \frac{v^R}{v_0} \quad \tilde{v}^\lambda \equiv \frac{v^\lambda}{v_0} \quad \tilde{v}^\varphi \equiv \frac{v^\varphi}{v_0}, \tag{55}$$

where T_0 $\left(=220\cdot 10^6\ \mathrm{yr}\right)$, r_0 $(=8500\ \mathrm{pc})$ and v_0 $(=12\ \mathrm{km/s})$ are appropriate scaling values.

In the dimensionless notation Eq. (55), the Eqs.(48) and (49) describing the Sun movement are:

$$
\begin{aligned}
&\dot{\tilde{R}}=\tilde{v}^R \qquad \dot{\lambda}=\frac{\tilde{v}^\lambda}{\tilde{R}\cos\varphi} \qquad \dot{\lambda}=\frac{\tilde{v}^\lambda}{\tilde{R}\cos\varphi}\\
&\dot{\tilde{v}}^R=\tilde{D}_1\frac{\left(\tilde{v}^\lambda\right)^2+\left(\tilde{v}^\varphi\right)^2}{\tilde{R}}-\tilde{D}_{2a}\frac{\tilde{R}}{\left(\tilde{B}^2+\tilde{R}^2\right)^{1/2}\left[\tilde{B}^2+\left(\tilde{B}^2+\tilde{R}^2\right)^{1/2}\right]^2}\\
&\qquad\qquad +\tilde{D}_{2b}\frac{2\tan^2(\varphi/2)}{\tilde{R}^3\left(1+D^2\tan^2(\varphi/2)\right)^{1/2}}+f^R\tilde{D}_3\\
&\tilde{v}^\lambda=-\tilde{D}_1\frac{\tilde{v}^R\tilde{v}^\lambda-\tilde{v}^\lambda\tilde{v}^\varphi\tan\varphi}{\tilde{R}}+f^\lambda\tilde{D}_3\\
&\dot{\tilde{v}}^\varphi=-\tilde{D}_1\frac{\tilde{v}^\lambda\tilde{v}^\varphi+\left(\tilde{v}^\lambda\right)^2\tan\varphi}{\tilde{R}}\\
&\qquad\qquad -\tilde{D}_{2b}\frac{1+\frac{D^2}{2}\tan^2(\varphi/2)}{\tilde{R}^3\left(1+D^2\tan^2(\varphi/2)\right)^{1/2}}\frac{\tan^2(\varphi/2)}{\cos^2(\varphi/2)}+f^\varphi\tilde{D}_3.
\end{aligned}
\tag{56a-e}
$$

Here the Eqs. (42) and (30) and the dimensionless parameters defined below were also used:

$$
\begin{aligned}
&\tilde{B}\equiv\frac{B}{r_0} \quad \tilde{D}_1\equiv\frac{v_0T_0}{r_0} \quad \tilde{D}_{2a}\equiv\frac{T_0A}{v_0r_0^2} \quad \tilde{D}_{2b}\equiv\frac{T_0C^2}{v_0r_0^3}\\
&\qquad\qquad \tilde{D}_3\equiv\frac{T_0}{v_0}\frac{L_s}{2c}\frac{1-\cos\Psi}{M_{sun}+M_{planets}}\left(1-e_{\mathrm{int}}\frac{\theta_p^4}{\theta_s^4}\right)
\end{aligned}
\tag{57}
$$

In Eqs. (56) the unit vector $\left(f^R, f^\lambda, f^\varphi\right)$ gives the direction of the thrust force per unit mass F' (see Eq. 42) in the coordinate system (R, λ, φ).

A simplifying hypothesis was adopted in Shkadov (1987) to allow an analytical solution for the perturbed motion of the Sun. Thus, one considered a particular set of initial conditions that makes the usual (unperturbed) motion of the Sun to be along a circular orbit in the equatorial plane $\varphi=0$ of the Galaxy. One proved that the ratio of the maximum acceleration generated by the Sun-mirror system to the Galaxy gravitational acceleration is less than one percent. One concluded that the magnitude of the thrust force is (relatively) small and the small parameter method can be used to solve the equations of the perturbed motion. Consequently, the perturbed motion of the Sun was described mathematically in Shkadov (1987) as a variational problem with respect to the unperturbed (circular) orbit.

In this chapter the Eqs. (56) are solved numerically by using the ODE-solver SDRIV3 from the SLATEC library (Fong et al., 1993).

A few details about the initial values used to solve the Eqs. (56) follow. The (absolute) Sun velocity is usually obtained by adding the (average) near circular velocity of the Galaxy at the Sun to the Sun's velocity in the local standard of rest (LSR). Discussions on various ways of defining the LSR can be found in (Bash, 1986, p. 42). One knows that the Sun is located near the corotation circle, where in a spiral galaxy such as ours the angular speeds of the spiral pattern and the stars are equal (Mishunov and Zenina, 1999). Consequently, one expects a rather small value for Sun's velocity in the LSR. Indeed, HIPPARCOS-based studies give the mean value 13.4 ± 0.4 km/s (Dehnen and Binney, 1998; Kovalevsky, 1999; Bienayme, 1999). The LSR velocity is higher for older than for younger stars due to accumulation of perturbations to a star's trajectory. Consequently, the present-day orbit differs from the originally nearly circular motion in plane (Gonzalez, 1999). One defines the Sun's velocity components (u, v, w) in the LSR as follow: u is the velocity positive outward away from the galactic center; v is the velocity in the galactic plane positive in the sense of the galactic rotation and w is the velocity in the direction perpendicular on the galactic plane, positive toward the north galactic pole (Bash, 1986, p. 36). In this convention $(u, v, w) = (0, 0, 0)$ characterizes a body at Sun position, moving in the galactic plane on a circular orbit. The initial components of LSR Sun velocity are denoted (u_0, v_0, w_0). In computation we used the rather popular values (in km/s):$(u_0, v_0, w_0) = (-9, 12, 7)$ (Bash, 1986, p. 36; Darling, 2004). The local components (U, V, W) of Galaxy's velocity are defined in a similar coordinate system, with the origin in the center of the Galaxy. One denotes by (U_0, V_0, W_0) the Galaxy's velocity at Sun position. In computations we used the values (in km/s): $(U_0, V_0, W_0) = (44, 235, 30)$ (Carlberg and Innanen, 1987). Therefore, the components of the initial (absolute) Sun velocity are: $v^R(t=0) = u_0 + U_0$, $v^\lambda(t=0) = v_0 + V_0$ and $v^\varphi(t=0) = w_0 + W_0$.

Note that the estimated Sun orbit is rather sensitive on the initial velocity. For example, in Bash (1986) the chosen values of both u_0 and v_0 were increased by 3 km/s and the orbit was integrated again. After 100 Myr the Sun's position was found to differ by 400 pc.

The initial coordinates of the Sun are as follows. At time $t = 0$ the Sun is found in the equatorial plane of the Galaxy. We thus have $\varphi(t=0) = 0$. This is reasonable as the Sun crosses the equatorial plane during its movement in the Galaxy (see e.g. Fig. 6a). Note that the present-day position of the Sun is estimated to about 10 to 20 pc above the equator plane (Pal and Ureche, 1983; Gonzalez, 1999), which is rather close to it. Other initial conditions are $\lambda(t=0) = 0$ and $R(t=0) = r_0$ (Carlberg and Innanen, 1987).

It is useful now to estimate how long one can safely integrate the Sun orbit. Indeed, the velocity dispersion of the Galaxy's disk stars increases with time, due to rather random encounters with interstellar clouds and periodical encounters with the spiral arms of stars. For example, during its lifetime the Sun has crossed the Galaxy's spiral arms about 17 times (Bash, 1986, p. 42). It may not be wise to

integrate the Sun's orbit, using a global potential, past one spiral arm's passage. Therefore, the time between spiral arm passages, which is about 260 Myr, is the maximum integration time accepted here.

First, the Eqs. (33) were solved in the case $f^R = f^\lambda = f^\varphi = 0$. This corresponds to the usual (unperturbed) motion of the Sun. Using the solution of Eqs. (33) one could obtain from Eqs. (47) the cartesian coordinates $x^i(t)$ $(i = 1, 2, 3)$ of the Sun on the unperturbed orbit. Second, the Eqs. (56) were solved in case the Sun motion is perturbed by the stellar engine thrust force. This requires of course using a non-null unit vector $\left(f^R, f^\lambda, f^\varphi\right)$ in Eqs. (56). The cartesian coordinates of the Sun on the perturbed orbit are denoted $x_p^i(t)$ $(i = 1, 2, 3)$.

Since the local force law is not inverse-square, the galactic orbit of the Sun is not expected to be a close Keplerian ellipse. The best-fitting, approximate, Keplerian ellipse to the Sun's current orbit shows $a \approx 1.07 r_0$ and $e \approx 0.07$, where a and e are the semi-major axis and the eccentricity of the orbit, respectively (Bash, 1986, p. 42). There is a reasonable concordance between these previous findings and the results obtained here (see Fig. 6a). The coordinate R lies between $0.903 r_0$ and $1.136 r_0$. A complete rotation of the Sun around the center of the Galaxy corresponds to a variation of λ between 0 and 360 degrees. It takes about 225 Myr. The Sun trajectory is placed both above and below the equatorial plane of the Galaxy (i.e. at positive and negative φ values, respectively) (Fig. 6a). The angular deviation from the equatorial plane is, however, small in absolute values (less than 5 degrees). The Sun trajectory crosses the equatorial plane two times during a complete rotation. One reminds that the simplified unperturbed Sun motion studied in Shkadov (1987) is confined to the equatorial plane of the Galaxy. A periodic oscillation motion in the lateral direction to the solar orbital plane was emphasized in the quoted paper only in case the Sun motion is perturbed by the mirror's thrust force.

Sun velocity changes on the unperturbed orbit (Fig. 6b). The tangential velocity v^λ has a monotonous time variation between apogalacticon and perigalacticon. The

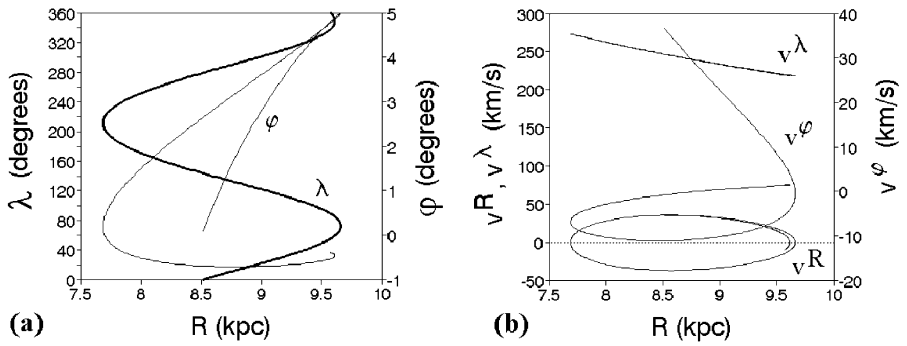

Figure 6. Solution of Eqs. (33) for one Sun revolution. (a) Dependence of angles λ and φ on R. (b) Dependence of Sun velocity components v^R, v^λ and v^φ on R

radial velocity v^R reaches its extreme values near $R = r_0$. The time variation of v^φ is slightly more complicated.

A stellar engine thrust force of constant magnitude will be considered in the following. The perturbed motion of the Sun depends, of course, on the direction of the thrust force. Three simple strategies of changing Sun movement are defined now. In the first case the thrust force is constantly acting on the (outward) direction of R and it corresponds to $f^R = 1,\ f^\lambda = f^\varphi = 0$ in Eqs. (56). The second case corresponds to $f^\varphi = 1,\ f^R = f^\lambda = 0$ and refers to a thrust force constantly acting on the direction of the generalized variable φ. A thrust force constantly acting on the direction of the generalized variable λ (i.e.$f^\lambda = 1,\ f^R = f^\varphi = 0$) is the third strategy.

In all the three above cases the time-dependent distance $\Delta R\,(t)$ between the perturbed and unperturbed positions of the Sun, respectively, is defined in the usual way as

$$\Delta R\,(t) \equiv \left[\left(x_p^1 - x^1\right)^2 + \left(x_p^2 - x^2\right)^2 + \left(x_p^3 - x^3\right)^2\right]^{1/2}. \tag{58}$$

The time dependence of ΔR is shown in Fig. 7 for the three strategies. A single rotation of the Sun around the center of the Galaxy was considered. The distance ΔR depends on the direction of the thrust force (i.e. on the strategy), as expected. None of the three strategies make the distance between the perturbed and the unperturbed Sun position increase linearly in time. An optimal control strategy for the thrust force direction is required for this purpose. The second strategy (i.e. $f^\lambda = 1$) yields the largest values of ΔR during the time interval considered here. The deviation from the unperturbed orbit could be as large as 40 pc. Note the maximum ΔR is obtained with the $f^R = 1$ strategy about 140 Myr after stellar engine implementation.

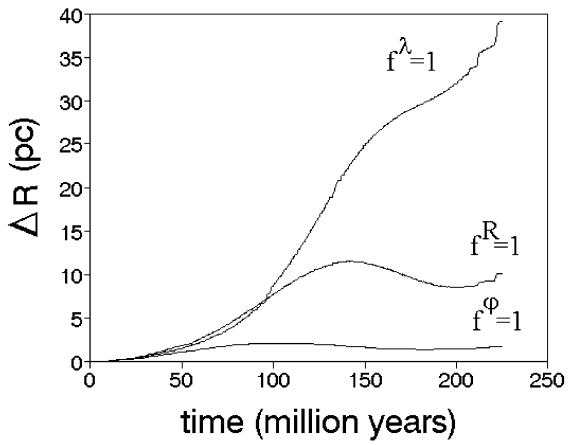

Figure 7. Time variation of distance $\Delta R\,(t)$ between the perturbed and unperturbed positions of the Sun, respectively, during one Sun galactic revolution. Solutions of Eqs. (56) were used. Three strategies of changing Sun movement are considered: (i) $f^R = 1$ (stellar engine thrust force is acting on the (outward) direction of R), (ii) $f^\lambda = 1$ (thrust force acting on the direction of λ), (iii) $f^\varphi = 1$ (thrust force acting on the direction of φ)

It is interesting to compare our findings with early results obtained in Shkadov (1987) by using a simplified analytical model. In the quoted paper the mirror axis forms a right angle with the radius-vector of the Sun that is assumed to move on a circular orbit in the equatorial plane of the Galaxy. This means that the thrust vector is always acting in the equatorial plane of the Galaxy and it is directed along the tangent to the solar orbit. In Shkadov (1987) the radius of the circular orbit of the Sun is estimated to 10 kpc while the period of one Sun revolution in the Galaxy is assumed to be 200 Myr. The quoted author found a Sun radial deviation from its orbit of about 12 pc. This is about three times smaller than the results obtained in this chapter by using a more accurate treatment.

4.3 Second Galaxy Gravitational Potential

Another axi-symmetric gravitational potential per unit mass of the solar system, $\Phi(r, \theta, z)$, will be used in this section. It consists of a disk-halo Plummer potential supplemented with some spherical potentials (see Carlberg and Innanen, 1987):

$$\Phi(r, \theta, z) = -\frac{\alpha_1 M_{eff} g}{\left\{\left[a + \sum_{i=1}^{3} \beta_i \left(z^2 + h_i^2\right)^{1/2}\right]^2 + b_1^2 + r^2\right\}^{1/2}} - \sum_{j=2}^{4} \frac{\alpha_j M_{eff} g}{\left(b_j^2 + r^2\right)^{1/2}}. \tag{59}$$

Here a cylindrical system of coordinates (r, θ, z) was used. Other notations in Eq. (59) are: g $\left(= 6.67 \cdot 10^{-11} \mathrm{m^3 kg^{-1} s^{-2}}\right)$ is the gravitational constant, $M_{eff} = 9.484 \cdot 10^{11} M_S$ is the effective Galaxy mass influencing Sun's movement, α_j $(j = 1, 2, 3, 4)$ are mass weighting coefficients for various potential components, a and b_1 are the scale length and the core radius of the disk-halo, respectively, β_i $(i = 1, 2, 3)$ and h_i $(i = 1, 2, 3)$ correspond to the scale heights of various disk-halo components while b_j $(j = 2, 3, 4)$ are the core radii of the additional spherical potentials (for bulge, nucleus and dark halo, respectively). Table 1 shows the data.

Table 1. Data for the Galaxy gravitational potential of (Carlberg and Innanen, 1987)

Component j	Disk-halo $(j = 1)$	Bulge $(j = 2)$	Nucleus $(j = 3)$	Dark-halo $(j = 4)$
α_j	0.1554	0.0490	0.0098	0.7859
b_j (kpc)	8.0	3.0	0.25	35.0
a (kpc)	3.0	0	0	0
β_1	0.4	0	0	0
β_2	0.5	0	0	0
β_3	0.1	0	0	0
h_1 (kpc)	0.325	0	0	0
h_2 (kpc)	0.090	0	0	0
h_3 (kpc)	0.125	0	0	0

The components of the gradient of Φ in the coordinate system (r, θ, z) are defined as projections of the gravitational acceleration vector G:

$$G^r = \frac{1}{H_r}\frac{\partial \Phi}{\partial r}, \quad G^\theta = \frac{1}{H_\theta}\frac{\partial \Phi}{\partial \theta} = 0, \quad G^z = \frac{1}{H_z}\frac{\partial \Phi}{\partial z}. \tag{60}$$

The Lamé coefficients H_i $(i = r, \theta, z)$ are used here. One denotes the components of Sun's velocity by v^i $(i = R, \lambda, \varphi)$ and one defines the new dimensionless variables:

$$\tilde{r} \equiv \frac{r}{r_0} \quad \tilde{v}^r \equiv \frac{v^r}{v_0} \quad \tilde{v}^\theta \equiv \frac{v^\theta}{v_0} \quad \tilde{v}^z \equiv \frac{v^z}{v_0}. \tag{61}$$

In the dimensionless notation Eqs. (61), the Eqs. (51)-(52) of Sun movement are:

$$\dot{\tilde{r}} = \tilde{D}_1 \tilde{v}^r \qquad \dot{\theta} = \tilde{D}_1 \frac{\tilde{v}^\theta}{\tilde{r}} \qquad \dot{\tilde{z}} = \tilde{D}_1 \tilde{v}^z \tag{62a-c}$$

$$\dot{\tilde{v}}^r = \tilde{D}_1 \frac{\left(\tilde{v}^\theta\right)^2}{\tilde{r}} + \tilde{D}_4 \left\{ \frac{\alpha_1 \tilde{r}}{\left\{ \left[\tilde{a} + \sum_{i=1}^{3} \beta_i \left(\tilde{z}^2 + \tilde{h}_i^2 \right)^{1/2} \right]^2 + \tilde{b}_1^2 + \tilde{r}^2 \right\}^{3/2}} + \sum_{j=2}^{4} \frac{\alpha_j \tilde{r}}{\left(\tilde{b}_j^2 + \tilde{r}^2 \right)^{3/2}} \right\} + f^r \tilde{D}_3 \tag{62d}$$

$$\dot{\tilde{v}}^\theta = -\tilde{D}_1 \frac{\tilde{v}^r \tilde{v}^\theta}{\tilde{r}} + f^\theta \tilde{D}_3 \tag{62e}$$

$$\dot{\tilde{v}}^z = \tilde{D}_4 \frac{\alpha_1 \tilde{z} \left[\tilde{a} + \sum_{i=1}^{3} \beta_i \left(\tilde{z}^2 + \tilde{h}_i^2 \right)^{1/2} \right]}{\left\{ \left[\tilde{a} + \sum_{i=1}^{3} \beta_i \left(\tilde{z}^2 + \tilde{h}_i^2 \right)^{1/2} \right]^2 + \tilde{b}_1^2 + \tilde{r}^2 \right\}^{3/2}} \left[\sum_{i=1}^{3} \frac{\beta_i}{\left(\tilde{z}^2 + \tilde{h}_i^2 \right)^{1/2}} \right] + f^z \tilde{D}_3 \tag{62f}$$

Here the Eqs. (42) and (59) and following dimensionless constants were also used:

$$\tilde{a} \equiv \frac{a}{r_0}, \quad \tilde{b}_1 \equiv \frac{b_1}{r_0}, \quad \tilde{h}_i \equiv \frac{h_i}{r_0} \ (i = 1, 2, 3), \quad \tilde{D}_4 \equiv \frac{T_0 M_{eff} g}{v_0 r_0^2}. \tag{63}$$

In Eqs. (62) the unit vector $\left(f^r, f^\theta, f^z\right)$ gives the direction of the thrust force F' (see Eq. 42) in the coordinate system (r, θ, z).

The Eqs. (62) are solved numerically by using the ODE-solver SDRIV3 (Fong et al., 1993). One assumes again that initially (i.e. at time $t = 0$) the Sun is found in the equatorial plane of the Galaxy. This makes possible to use the same initial conditions we used in Section 4.1. In cylindrical coordinates, this means $r\,(t = 0) = r_0$, $\theta\,(t = 0) = 0$ and $z\,(t = 0) = 0$. The components of the initial Sun velocity are: $v^r\,(t = 0) = u_0 + U_0$, $v^\theta\,(t = 0) = v_0 + V_0$ and $v^z\,(t = 0) = w_0 + W_0$.

To solve the unperturbed motion of the Sun requires using $f^r = f^\theta = f^z = 0$ in Eqs. (62). Results are shown in Fig. 8. The coordinate r lies between $0.942r_0$ and $1.193r_0$. This is in reasonably good agreement with results given in Bash (1986), where an approximate Sun motion confined to the galactic mid-plane was studied. A perturbation potential due to standard spirals pattern was however included in that model. The perturbation potential was assumed to be 5% of the global axi-symmetric potential. The initial values were slightly different from those we used here. One found that the Sun reaches perigalacticon at $r = 0.995\hat{r}_0$ and apogalacticon at $r = 1.145\hat{r}_0$, where $\hat{r}_0$ is the initial value of r used in Bash (1986).

A complete rotation of the Sun around the center of the Galaxy (that corresponds to a variation of θ between 0 and 360 degrees) takes about 248.5 Myr. This is about 10 % longer than in case of the gravitational potential used in section 4.1.

The rotation motion of the Sun is qualitatively similar for both Galaxy gravitational potentials we considered in this paper (compare Fig. 8 and Fig. 6, respectively). Differences exist however in the predictions about the vertical motion.

A usual simplified orbit integration procedure is to separate the motion in the mid-galactic plane from the Sun's vertical motion. Sometimes the last motion is modeled as a simple harmonic oscillation. A vertical oscillation period of 66 Myr was accepted, for example, in Bash (1986). In this case the Sun would cross the mid-plane every 33 Myr, i.e. between seven and eight times during a complete revolution.

In the present work there is no decomposition of Sun motion and, therefore, more accurate results are expected. Figure 8a shows that the Sun deviation from the equatorial plane of the Galaxy lies between -80 pc and $+80$ pc and the Sun trajectory crosses the equatorial plane four times during a complete revolution.

Note that in Gonzalez (1999) one estimates that the Sun spends most of its time at least 40 pc from the Galactic mid-plane. Also, some studies reported for the maximum distance $z_{\max}$ between the Sun and Galaxy's equatorial plane values ranging from 76.8 to 81.8 pc (Bash, 1986), which is in good concordance with our results.

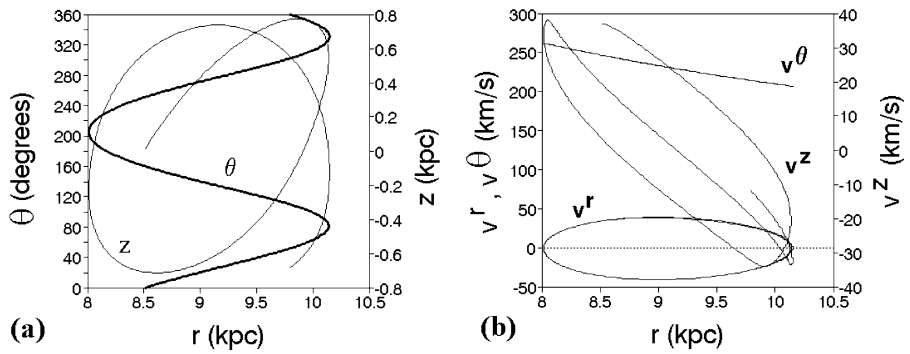

Figure 8. Solution of Eqs. (62) for one Sun revolution. (a) Dependence of variables θ and z on r. (b) Dependence of Sun velocity components v^r, v^θ and v^z on r

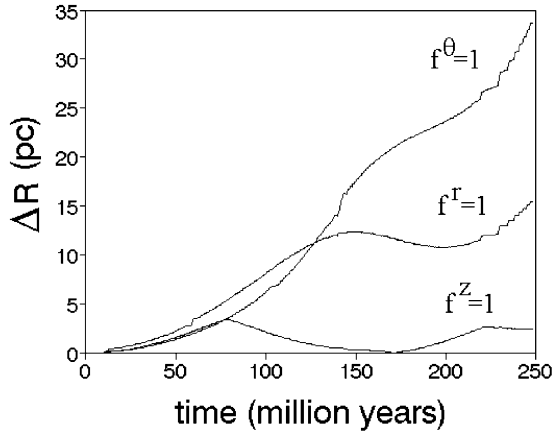

Figure 9. Time variation of the distance $\Delta R\,(t)$ between the perturbed and unperturbed positions of the Sun, respectively, during one Sun galactic revolution. Solutions of the equations system (62) were used. Three strategies of changing Sun movement are considered: (i) $f^r = 1$ (stellar engine thrust force is acting on the (outward) direction of r), (ii) $f^\theta = 1$ (thrust force acting on the direction of the generalized variable θ), (iii) $f^z = 1$ (thrust force acting on z direction)

The tangential velocity v^θ and the radial velocity v^r have a monotonous time variation between their minimum and maximum values but the time variation of v^z is slightly more complicated (Fig. 8b).

Three simple strategies of changing Sun movement are again considered here. In the first case the stellar engine thrust force is constantly acting on the (outward) direction of r and it corresponds to $f^r = 1,\ f^\theta = f^z = 0$ in Eqs. (62). The second case corresponds to $f^\theta = 1,\ f^r = f^z = 0$ and refers to a thrust force constantly acting on the direction of the generalized variable θ. A thrust force acting on z direction (i.e. $f^z = 1,\ f^r = f^\theta = 0$) is the third strategy.

The time-dependent distance $\Delta R\,(t)$ between the perturbed and unperturbed positions of the Sun is defined by Eq. (58).

Figure 9 shows the time dependence of ΔR during one Sun revolution for the three strategies defined above. The second strategy (i.e. $f^\theta = 1$) yields the largest values of ΔR. The maximum deviation from the unperturbed orbit is about 35 pc. This is in good agreement with the result obtained by using the gravitational potential of section 4.1 (compare Fig. 9 and Fig. 7, respectively).

5. CONCLUSIONS

A stellar engine is defined in this chapter as a device that uses an important part of star resources to produce work. A classification is proposed as follows. A class A stellar engine uses *the impulse* of the radiation emitted by a star to produce a thrust force. When acting on a finite distance the thrust force generates work. Class A stellar engines can be used for interstellar travel. As example we quote the Sun

thruster proposed by Shkadov (1987). A class B stellar engine uses *the energy* of the radiation emitted by a star to generate mechanical power. It is based on the concept of the Dyson sphere (DS). As example we cite the stellar engine proposed in Badescu (1995). A class C stellar engine is a combination between class A and class B stellar engines and provides a Kardashev type II civilisation with both power and the possibility of interstellar travel.

A class A stellar engine is associated with an increase in the affected star's photosphere temperature. For instance, by increasing the mirror's rim angle from 0 to 90 degrees the spectral class of the Sun changes from G2 towards F2. However, a reasonable rim angle value ($\Psi = 30°$) keeps the photosphere temperature (and its associated spectral class) quite close to the present-day values.

A number of conclusions may be drawn regarding the manufacturing of a class B stellar engine in our solar system. First, small radii increase the feasibility of the project as the amount of material required is proportional to the square of the radius. Second, the inner planets seem to be the best source of material because of the shorter distance between their orbit and the place of the future construction.

The efficiency of a class C stellar engine increases by increasing its radius and decreasing the mirror rim angle Ψ. There is a minimum radius for such engine to provide useful power. The important fact is that there is an optimum stellar engine radius as far as the provided power density is concerned. For values adopted here this optimum radius is around 450 millions km (see Fig. 4c).

The mirror of class A and class C stellar engines makes the Sun's temperature increase and this has consequences on the thrust force acting on the Sun. In both cases the thrust force F increases by increasing the mirror rim angle Ψ, as expected. The thrust force of the class A stellar engine is, however, larger than first estimated by Shkadov (1987) without taking into account the increase in the Sun's temperature.

Changing into a controllable way the trajectory of the Sun in the Galaxy is of great potential interest for humanity. In this chapter we have studied in some detail how class A or class C stellar engines could be used for this purpose. One has proved in Section 3.4 that both types of stellar engines provide practically the same thrust force when used to change Sun orbit.

A simple dynamic model for Sun motion in the Galaxy was developed in Section 4. It takes into account the (perturbation) thrust force provided by the stellar engine, which is superposed on the usual gravitational forces. The model allowed us to evaluate the distance between the perturbed position of the Sun and the usual Sun position. To increase confidence in results two different Galaxy gravitational potential models were used in calculations. In both cases, the results obtained show similar qualitative features for Sun's unperturbed motion.

Three simple strategies of changing Sun orbit were considered. A constant module thrust force was always assumed and the difference consisted in the force direction. None of these strategies make the distance between the perturbed and the unperturbed Sun position increase linearly in time. For this purpose an optimal control strategy is to be used.

For a single Sun revolution the maximum estimated deviation is between 35 and 40 pc (depending on the gravitational potential involved). Both Fig. 7 and Fig. 9 show that the stellar engine gives a 10 pc deviation of the Sun in less than 150 Myr. The number density of stars in the solar neighborhood is about 0.104 per cubic pc and so within a 10 pc radius sphere we would find around 400 stars, about 10 of which would be single solar-type stars (see e.g. (Fogg, 1995, p. 461)). This gives some perspective to future interstellar transfer macro-projects. The duration involved is, however, large and other kinds of stellar engines than those we studied must also be considered. One concludes that class A or class C stellar engines may be used to control in a certain extent the Sun's movement in the Galaxy.

ACKNOWLEDGMENTS

This work is dedicated to our friend Henrik Farkas (Technical University of Budapest) who passed away on 21 July 2005.

REFERENCES

Badescu V (1993) Maximum concentration ratio of direct solar radiation. Appl Optics 32(12):2187–2189

Badescu V (1995) On the radius of the Dyson sphere. Acta Astronautica 36:135–138

Badescu V (2004) Simulation of a solar Stirling engine operation under various weather conditions on Mars. J Solar Energy Eng 126:812–818

Badescu V, Cathcart RB (2000) Stellar engines for Kardashev's type II civilisations. J Br Interplanet Soc 53:297–306

Badescu V, Cathcart RB (2006) Use of class A and class C stellar engines to control sun movement in the galaxy. Acta Astronautica 58:119–129

Bash F (1986) The present, past and future velocity of nearby stars: the path of the Sun in 10^8 years. In: Smoluchowski R, Bahcall JN, Matthews MS (eds) The Galaxy and the Solar System. The University of Arizona Press, Tucson

Bejan A (1996) Entropy generation minimization: the new thermodynamics of finite-size devices and finite-time processes. J Appl Phys 79:1191–1218

Beju I, Soos E, Teodorescu PP (1976) Tehnici de Calcul Vectorial Cu Aplicatii, Editura Tehnica, Bucuresti

Bienayme O (1999) The local stellar velocity of the galaxy: galactic structure and potential. Astronomy Astrophysics 341:86–97

Carlberg RG, Innanen KA (1987) Galactic chaos and the circular velocity at the sun. Astron J 94:666–670

Clube SVM, Napier WM (1984) Terrestrial catastrophism: Nemesis or galaxy? Nature 311:635–636

Criswell DR (1985) Solar system industrialization: implications for interstellar migrations. In: Finney R, Jones EM (eds) Interstellar Migration and the Human Experience. University of California Press, Berkeley, pp 50–87

Darling D (2004) The Universal Book of Astronomy. Wiley, New York, pp 456

De Vos A (1985) Efficiency of some heat engines at maximum-power conditions. Am J Phys 53(5):570–573

Dehnen MW, Binney JJ (1998) Local stellar kinematics from HIPPARCOS data. Monthly Notices Royal Astronom Society 298:387–394

Dyson FJ (1966) The search for extraterrestrial technology. In: Marshak RE (ed) Perspectives in modern physics. Interscience Publishers, New York, pp 641–655

Fogg MJ (1989) Solar exchange as a means of ensuring the long term habitability of the Earth. Spec Sci Technol 12:153–157

Fogg MJ (1995) Terraforming: Engineering Planetary Environments. SAE, Warrendale
Fong KW, Jefferson TH, Suyehiro T, Walton L (1993) Guide to the SLATEC common mathematical library. Energy Science and Technology Software Center, PO Box 1020, Oak Ridge, TN 37831, USA
Gonzalez G (1999) Is the Sun anomalous? Astronomy Geophys 40:5.25–5.25.29
Hills JG (1984) Close encounters between a star-planet system and a stellar intruder. Astron J 89:1559–1564
Hoffmann KH, Burzler JM, Schubert E (1997) Endoreversible Thermodynamics. J Non-Equilib Thermodyn 22:311–355
Infante F (1992) Projects for the reconstruction of the firmament. Leonardo 25:11
Jones EM (1981) Discrete calculations of interstellar migration and settlement. Icarus 46:328–336
Kardashev NS (1964) Transmission of information by extraterrestrial civilisations, Astron Zh 8:217
Kasting JF (1988) Runaway and moist greenhouse atmospheres and the evolution of Earth and Venus. Icarus 74:472–494
Knill O (2003) Moving the solar system. http://www.dynamical.systems.org/zwicky/Essay.html
Korykansky DG (2004) Astroengineering, or how to save the Earth in only one billion years. Rev Mex A A (Serie Conferencias) 22:117–120
Korykansky DG, Laughlin G, Adams FC (2001) Astronomical engineering: a strategy for modifying planetary orbits. Astrophys Sp Sci 275:349–366
Kovalevsky J (1999) First results from HIPPARCOS. Annu Rev Astronomy Astrophys 36:99–130
Landsberg PT, Badescu V (1998) Solar energy conversion: list of efficiencies and some theoretical considerations. Part I – Theoretical considerations. Prog Quantum Electronics 22:211–230
McInnes CR (2002) Astronomical engineering revisited: planetary orbit modification using solar radiation pressure. Astrophys Sp Sci 282:765–772
Mishunov Yu N, Zenina IA (1999) Yes, the Sun is located near the corotation circle. Astronomy Astrophys 341:81–85
Moore P (1970) Atlas of the Universe. Mitchell Beazley Ltd, London, pp 35,155,159,169
Nakajima S, Hayashi YY, Abe Y (1992) A study of the 'runaway greenhouse effect' with a one-dimensional radiative convective equilibrium model. J Atmos Sci 49:2256
Napier WN (1985) Comet formation in molecular clouds. Icarus 62:384
Newman WI, Sagan C (1981) Galactic civilizations: population dynamics and interstellar diffusion. Icarus 46:293–327
Pal A, Ureche V (1983) Astronomie. Ed. Didactica si Pedagogica, Bucharest, pp. 161
Sackmann I-J, Boothroyd AI, Kraemer KE (1993) Our Sun III: Present and future. Astrophys J 418:457
Shkadov LM (1987) Possibility of controlling solar system motion in the galaxy. 38th Congress of IAF, paper IAA-87–613. Brighton, UK, October 10–17
Ureche V (1987) Universul. Astrofizica, vol 2. Dacia, Cluj-Napoca
Zuckerman B (1985) Stellar evolution: motivation for mass interstellar migrations. Q J R Astr Soc 26:56–59
Zwicky F (1957) Morphological astronomy. Springer-Verlag, Berlin, pp. 260